DIFFERENT STICTION MECHANISMS IN ELECTROSTATIC MEMS DEVICES: NANOSCALE CHARACTERIZATION BASED ON ADHESION AND FRICTION MEASUREMENTS

U. Zaghloul[1,2,3], B. Bhushan[3], P. Pons[1,2], G. Papaioannou[1,2,4], F. Coccetti[1,2,5], and R. Plana[1,2]*
[1]CNRS; LAAS; 7 avenue du colonel Roche, F-31077 Toulouse, France
[2]Université de Toulouse; UPS, INSA, INP, ISAE ; LAAS ; F-31077 Toulouse, France
[3]NLBB Laboratory, The Ohio State University, Columbus, OH 43210, USA
[4]University of Athens, Solid State Physics, Panepistimiopolis Zografos, Athens, Greece
[5]Novamems, 10 avenue De l'Europe, F-31520 Toulouse, France

ABSTRACT

In this work, different stiction mechanisms in electrostatic micro-electromechanical systems (MEMS) and particularly in RF-MEMS switches were studied for the first time. In these devices stiction can be caused by two main mechanisms: dielectric charging and meniscus formation resulting from the adsorbed water film between the switch bridge and the dielectric layer. The effect of each mechanism and their interaction were investigated by measuring the adhesive and friction forces under different electrical stress conditions and relative humidity levels. An atomic force microscope (AFM) was used to perform force-distance and friction measurements on the nanoscale. The study provides an in-depth understanding of different stiction mechanisms, and explanation for the literature reported lifetime measurements for electrostatic capacitive MEMS switches.

KEYWORDS

Stiction; dielectric charging; adhesive force, field-induced meniscus; friction force; electrostatic MEMS

I. INTRODUCTION

Among various reported reliability concerns for electrostatic capacitive MEMS switches, the dielectric charging and its resulting stiction is considered the main failure mechanism of these devices [1-4]. On the other hand, capillary condensation of water vapor results in the formation of meniscus bridges between contacting and near-contacting asperities of two surfaces in close proximity to each other. This leads to an intrinsic attractive force which may lead to high adhesion and stiction [5]. The meniscus formation is also reported to be highly affected by the electric filed [6, 7]. Thus, the voltage used to actuate MEMS switches and the resulting dielectric charging are expected to affect the meniscus formation at the interface between the switch bridge and the dielectric film. Therefore, the adhesion or stiction between the switch bridge and the dielectric film could be also affected by the meniscus formation. The individual impact of the two different stiction mechanisms (charging induced and meniscus force induced) and their interaction under different operating conditions are not understood and have not been studied before.

This study presents a novel characterization technique to study different stiction mechanisms in electrostatic MEMS switches. The proposed methodology uses the AFM tip to simulate a single asperity contact with the dielectric surface [1, 2]. Force-distance and friction experiments were performed on the nanoscale and were used to measure the adhesive force and friction force, respectively, under different humidity levels and electrical stress conditions. The induced surface potential over the dielectric surface was measured, and was used to explain the obtained results.

II. EXPERIMENTAL DETAILS

The investigated samples consist of PECVD SiN_x films with 300 nm thickness deposited over 500 nm Au layers, which were evaporated over Si substrates (see sub figure in Fig. 1). In order to separately study the influence of meniscus formation, adhesion and friction experiments were performed under different relative humidity levels. Then, for each humidity level the adhesive and friction forces were measured while different bias amplitudes were applied to the Au layer underneath the SiN_x film. Due to this applied voltage, the SiN_x film is charged and hence the adhesion and friction induced by the dielectric charging could be assessed.

Force-distance experiments were used to measure the adhesive force between the AFM tip and the SiN_x film as well as the adsorbed water film thickness over the SiN_x surface [5]. An example of the force-distance curve for the investigated samples is presented in Fig. 1. The force-distance measurement starts at a large separation (point A) where there is no deflection of the cantilever. As the piezo moves towards the sample, a sudden mechanical instability occurs between point B and point C, and the tip jumps into contact with the adsorbed water film and wicks up around it to form a meniscus. The cantilever bends downwards because of the attractive meniscus force acting on the tip. As the piezo further approaches the SiN_x surface, the deflection of the cantilever increases while the tip travels in the water film and eventually contacts the underlying SiN_x surface at point C, and then the cantilever starts to bend upwards. Once the piezo reaches the end of its designated ramp size at point D, it is retracted to its starting position. The tip goes beyond zero deflection (point E) and enters the adhesion region. At point E, the elastic force of the cantilever becomes equivalent to the adhesive force, causing the cantilever to snap back to point F. The piezo travel distance used in this study is 500 nm which is comparable to the normal air gap of MEMS switches. The adhesive force, which is the force needed to pull the tip away from the sample, is calculated from the force distance curve by multiplying the vertical distance between E and F with the cantilever stiffness (Fig. 1). Also, the adsorbed water film thickness is the sum of the cantilever deflection (h_1) and the piezo travel distance (h_2) as highlighted in Fig. 1.

Friction force measurements were conducted by scanning the AFM tip orthogonal to the cantilever axis over a scan length of 10 μm. The normal load was varied

(35-990 nN), and a friction force measurement was taken at each increment. The friction force is given by [5]

$$F_{friction} = \mu(W + F_{adhesive}) \quad (1)$$

where μ is the coefficient of friction, W is the applied normal load, and $F_{adhesive}$ is the adhesive force.

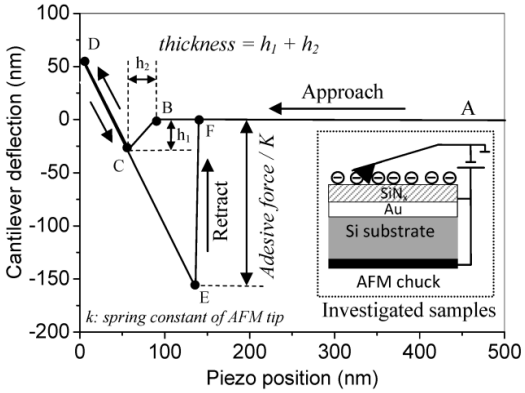

Figure 1: Force-distance curve for the investigated samples.

III. RESULTS AND DISCUSSION

Effect of Meniscus Force When No Bias Is Applied

Figure 2a shows that the adhesive force increases considerably when the relative humidity (RH) increases from 1% to only 20%, and the increase tends to saturate at larger RH. The measured thickness of the adsorbed water film over the SiN_x surface also increases with humidity as highlighted in the figure. The increase of the water film thickness enhances the meniscus formation, and consequently results in increasing the adhesive force. Though the measured increase in the water film thickness when increasing the humidity from 1% RH to 80% RH is found to be relatively small, the adhesive force increases considerably. In addition, when humidity increases, the meniscus becomes easier to form and more difficult to rupture [8]. This leads to stronger attractive capillary force between the tip and the sample, and hence larger adhesive force with increasing the humidity. Figure 2b highlights that the coefficient of friction, μ, increases sharply when increasing the RH from 1% to only 10%. This increase is attributed to the considerable increase in the adhesive force measured at 10% as presented in Fig. 2a. When RH increases beyond 10% RH, μ is found to decrease in spite of the measured increase in the adhesive force in this humidity range. This indicates that at larger RH the water film acts as a lubricant material [5]. The considerable change in the adhesive force and μ when RH increases to only 20% and 10%, respectively, indicates that the SiN_x material is very sensitive to any tiny amount of water molecules adsorbed over its surface.

Effect Of Applied Bias

The separate and combined effect of the two mentioned stiction mechanisms were studied by using three different groups of SiN_x samples (A, B, and C) which have the layer structure shown in Fig. 1. Group A and B were dehydrated just before performing the experiments through two cycles of heating (150 °C) and cooling steps under vacuum. This removes a considerable amount of the adsorbed water over the dielectric surface. Then, group A was measured under a very low RH level (1%), while group B was stored under high RH (60%) for 60 min, and then was measured under 60% RH. Group C was not dehydrated, and was measured under a low humidity level (1%) similar to group A. The thickness of the adsorbed water layer for group A is therefore smaller than groups B and C. Consequently, the contribution of the meniscus force to the measured adhesive is expected to be much smaller for group A compared to groups B and C. Comparing groups A and B, the influence of the water molecules adsorbed during 60 min under high relative humidity (60%) could be assessed. Also, the comparison between groups A and C reveals the influence of the annealing step.

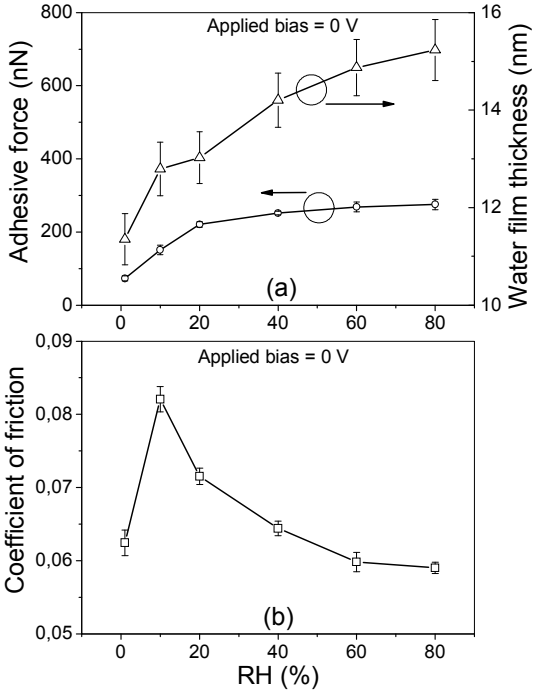

Figure 2: The effect of the relative humidity on (a) adhesive force and water film thickness, and (b) coefficient of friction.

Figure 3 presents the measured adhesive force under different applied bias for the three sample groups. For the three groups, the adhesive force is found to increase with the applied bias. This increase is attributed to the increase in the attractive electrostatic force between the AFM tip and the SiN_x surface as the applied bias increases. The increase in the adhesive force with bias is found to be very small for group A compared to groups B and C. In these experiments, the adhesive force was measured while the bias is applied between the AFM tip and the sample. Since the SiN_x film is charged and this results in an induced potential over the dielectric surface, the effective applied bias between the AFM tip and the sample is reduced. The induced surface potential over the SiN_x surface for the three groups of samples was measured, and the effective applied bias was calculated, and plotted in Fig. 3.

For a given applied bias, the effective bias is much smaller for group B compared to group A as presented in Fig. 3. Therefore, the electrostatic attractive force for group B is much smaller than group A for all investigated applied bias. In spite of that, the adhesive force measured

under different bias for group B is found to be much larger compared to group A. Thus, the difference in the trend of the adhesive force versus the applied bias between both groups cannot be attributed to the electrostatic attractive force. Additionally, the relatively small difference in the adhesive force between the two groups when no bias is applied (also shown in Fig. 2a) clearly indicates that the large difference between both groups at higher bias cannot be explained by the liquid mediated meniscus formation. Since the individual impact of the attractive electrostatic force and the liquid mediated meniscus formation does not explain the high difference in the adhesive force between groups A and B, there must be other adhesion mechanisms.

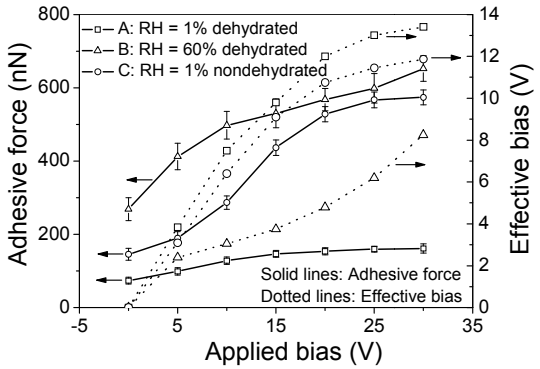

Figure 3: The impact of applied bias on adhesive force.

There are different mechanisms for the meniscus formation. When mechanical instability occurs (between points B, C in Fig. 1), the tip forms a liquid mediated meniscus with the adsorbed water film (Fig. 4a). It is also reported that the water film between the AFM tip and the sample surface grows under the influence of the electric field, forming a meniscus that becomes unstable when a critical field is reached [6, 7]. At this point, the meniscus suddenly forms a bridge between the tip and surface as shown in Fig. 4b. This is called a field-induced meniscus. A modeling study shows that the height of the water film under the tip almost doubles upon the formation of the field-induced meniscus [6]. Therefore, the increase in the water film thickness caused by field-induced meniscus is much higher compared to the increase in the water film thickness caused by increasing the humidity (see Fig. 2a). Also, due to the attraction of water molecules towards the tip under electric field, the volume of the meniscus surrounding the tip will increase considerably. As a result, the field-induced meniscus and its resulting increase in the water volume surrounding the tip will result in increasing the adhesive force between the AFM tip and sample surface remarkably. For these reasons, the influence of the field-induced meniscus on the adhesive force is expected to be much larger compared to the effect of the liquid mediated meniscus. The threshold voltage required to induce the formation of water bridges between a metallic tip and a flat metallic sample is given by [7].

$$V_{th} = 3.5D\sqrt{\ln(1/RH)} \qquad (2)$$

where D is the distance at which the field-induced meniscus forms, and RH is the employed relative humidity. Based on Eq. 2, for a given tip-sample separation, the required threshold voltage for the formation of water bridges decreases considerably when humidity increases.

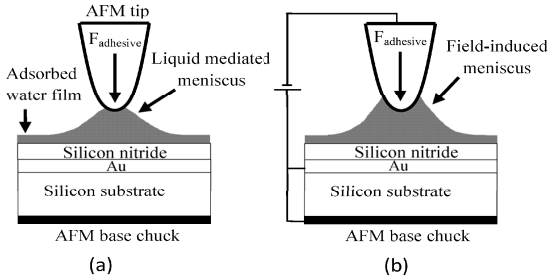

Figure 4: Different mechanisms of meniscus formation between the AFM tip and the sample surface.

Figure 3 shows that for sample group B the adhesive force increases considerably at relatively small effective bias (around 5 V). Based on the previous analysis, this increase is attributed to the field-induced meniscus, and it indicates that the threshold field has been reached. This is supported by the small calculated value of the threshold voltage at 60% RH from Eq. 2 which is 8.2 V. In addition, higher RH would lead to a stronger attractive capillary force since the adhesive force becomes longer ranged. According to that, the field-induced meniscus can persist at a longer tip-sample separation before bridge rupture [8]. Therefore the adhesive force measured at 60% RH (group B) will increase considerably by the field-induced meniscus formation. The smaller increase in the adhesive force with the applied bias for sample group A compared to group B indicates that the threshold field has not been reached for group A. Figure 3 also highlights that the increase in the adhesive force with the applied bias for sample group C is much higher compared to group A. Also, the effective applied bias, hence, the electrostatic force, is relatively smaller for group C compared to group A. Therefore, the higher increase rate of adhesive force with the applied bias for group C compared to group A cannot be explained by the liquid mediated meniscus and/or by the electrostatic attractive force. Obviously, the difference between both groups is attributed to the field-induced meniscus formation. The adsorbed water film thickness over the dielectric surface for group C is larger compared to group A due to the dehydration step performed for group A. Apparently, the thicker adsorbed water film in group C enhances the field-induced meniscus formation.

The friction force is found to increase exponentially with the applied bias for different applied mechanical normal loads and for both groups A and B as shown in Fig. 5a. Also, the trend of the friction force as a function of the applied bias for both groups is found to be very close. From Eq. 1, the friction force increases with the adhesive force which increases with the applied bias (Fig. 3). As the applied bias increase, the mechanical normal load between the tip and the sample surface also increases due to the lager attractive electrostatic force. The additional normal load under different applied bias was measured and was found to increase exponentially with the applied bias as shown in Fig. 5b. Thus, the linear

relation between the friction force and the normal load (Eq. 1) explains the exponential increase in the friction force with the applied bias as presented in Fig. 5a. The calculated coefficient of friction under different applied bias for groups A and B is shown in Fig. 5b. It is clear that the applied bias has a minimal impact on the coefficient of friction for both groups compared to the influence of relative humidity (Fig. 2b). In addition, the difference in the coefficient of friction calculated for both groups is found to be small for all applied bias values. This is attributed to the lubricant behavior of the adsorbed water layer in group B [5]. Comparing Fig. 3 and Fig. 5a, the applied bias and hence the dielectric charging affects mainly the adhesive force and not the friction force. Therefore, it is concluded that the adhesive force and not the friction force is the main force component which determines the lifetime of electrostatic MEMS switch.

Three categories of MEMS switches (switch-A, switch-B and switch-C) are assumed, which employ the sample groups A, B and C, respectively. Based on the previous discussion, the adhesion or stiction between the switch bridge and the dielectric will be much faster in switch-B compared to switch-A. This explains why MEMS switches operated at larger humidity levels have shorter lifetimes as reported in [4]. Also, stiction in switch-C will be much faster compared to switch-A, and this explains why annealing MEMS switches increases the device lifetime as reported in [3]. For switch-B and C, the main stiction mechanism is the field-induced meniscus formation enhanced by the dielectric charging. For MEMS switch-A, if the induced surface potential reaches the critical threshold, field-induced meniscus will be formed, and the high resulting adhesive force will cause the switch stiction. Otherwise, the stiction will be caused by the electrostatic attractive force.

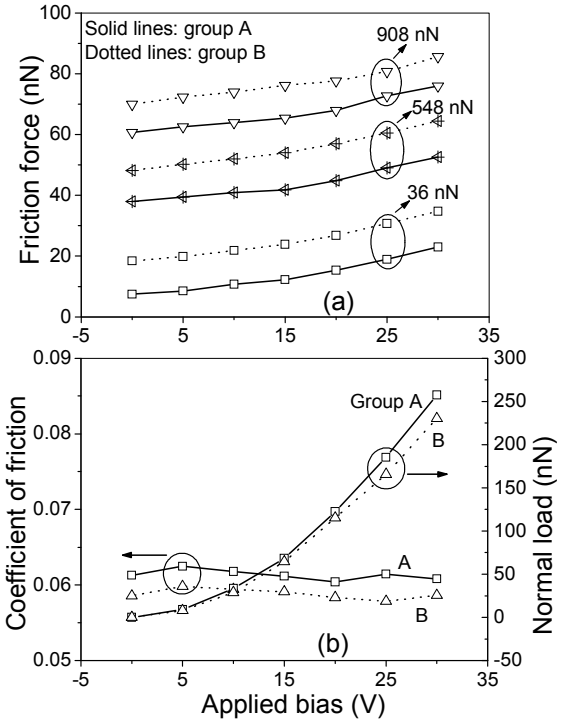

Figure 5: The impact of the applied bias on friction force and coefficient of friction.

IV. CONCLUSION

The adhesive force induced by meniscus formation due to the adsorbed water layer is found to be relatively small when the dielectric layer is not electrically stressed. When voltage is applied, the adhesive force increases considerably for dielectric films which have not been annealed even after being measured at a very low humidity level, due to the field-induced meniscus. For the annealed samples, the contribution of the field-induced meniscus is very high when the sample is stored under larger relative humidity for a short time. This study explains well why MEMS switches operated at larger relative humidity have shorter lifetimes and why annealing MEMS switches increases the device lifetime.

REFERENCES

[1] U. Zaghloul, G. J. Papaioannou, F. Coccetti, P. Pons and R. Plana, "A systematic reliability investigation of the dielectric charging process in electrostatically actuated MEMS based on Kelvin probe force microscopy," J. Micromech. Microeng. vol. 20, Art.# 064016, 2010.

[2] U. Zaghloul, G.J. Papaioannou, H. Wang, B. Bhushan, F. Coccetti, P. Pons, and R. Plana, "Nanoscale characterization of the dielectric charging phenomenon in PECVD silicon nitride thin films with various interfacial structures based on Kelvin probe force microscopy," Nanotechnology Vol. 22, Art. # 205708, 2011.

[3] P. Czarnecki, X. Rottenberg, P. Soussan, P. Ekkels, P. Muller, P. Nolmans, W. De Raedt, H. Tilmans, R. Puers and L. Marchand, "Effect of substrate charging on the reliability of capacitive RF MEMS switches," Sens. Actuator A-Phys. vol. 154, pp. 261-268, 2009.

[4] W. Van Spengen, P. Czarnecki, R. Poets, J. Van Beek and I. De Wolf, "The influence of the package environment on the functioning and reliability of RF-MEMS switches," Proc. IEEE IRPS, pp. 337-341, 2005.

[5] B. Bhushan, "Nanotribology and Nanomechanics - An Introduction," 3rd edition, Springer-Verlag, Heidelberg, Germany, 2011.

[6] S. Gómez-Monivas, J. J. Sáenz, M. Calleja, and R. Garcia, "Field-induced formation of nanometer-sized water bridges," Phys. Rev. Lett. vol. 91, 056101, 2003.

[7] G. Sacha, A. Verdaguer, and, M. Salmeron, " Induced water condensation and bridge Formation by electric fields in Atomic Force Microscopy," J. Phys. Chem. B, vol. 110, pp. 14870-14873, 2006.

[8] M. Yumei, X. Zhang, W. Wang, "Capillary liquid bridges in atomic force microscopy: Formation, rupture, and hysteresis," J. Chem. Phys. vol. 131, 184702, 2009.

CONTACT

*Usama Zaghloul, tel: +33-5-6133-6817; usama.zaghloul@laas.fr